

Imaginary chemical potential quantum Monte Carlo for Hubbard molecules

Fei Lin, Jurij Smakov, Erik S. Sørensen, Catherine Kallin and A. John Berlinsky

Department of Physics and Astronomy, McMaster University, Hamilton, Ontario, Canada L8S 4M1

(Dated: March 22, 2024)

We generalize the imaginary chemical potential quantum Monte Carlo (QMC) method proposed by Dagotto et al. [Phys. Rev. B 41, R811 (1990)] to systems without particle-hole symmetry. The generalized method is tested by comparing the results of the QMC simulations and exact diagonalization on small Hubbard molecules, such as tetrahedron and truncated tetrahedron. Results of the application of the method to the C_{60} Hubbard molecule are discussed.

PACS numbers: 71.10.Li, 02.70.Ss, 74.70.Wz

I. INTRODUCTION

Knowledge of the evolution of energy levels with doping in strongly correlated systems is of significant importance for understanding the physical mechanisms leading to their unconventional properties. For example, information about the changes in the ground state energy of model electron systems (such as Hubbard model) upon electron or hole doping may be used to confirm or disprove hypotheses about the origin of the pairing mechanism, eventually leading to superconductivity. Accessing this information analytically usually requires the use of various approximations, numerical techniques are often the only tools which can provide unbiased estimates for the observables of interest.

We have recently applied the auxiliary field quantum Monte Carlo (AFQMC) on a C_{60} molecule to extract the electronic binding energies [1]. AFQMC has been widely used in Hubbard Hamiltonian simulations since its introduction by Blankenbecler et al. [2, 3], and its further development by Hirsch [4] and White et al. [5]. Being a finite-temperature technique, AFQMC does not allow easy access to the physical observables, not represented by thermodynamic averages, such as energy gaps. A convenient procedure to extract this additional information from the AFQMC data was proposed by Dagotto et al. [6], who introduced imaginary chemical potentials in AFQMC simulations. It was then used to extract the charge gaps of the one-band Hubbard model on finite two-dimensional (2D) square lattices.

In the present paper we generalize this formalism to systems without particle-hole symmetry, such as the tetrahedron, truncated tetrahedron and C_{60} molecules. The canonical partition function ratios are obtained from the expansions of the AFQMC determinant ratios for a set of finite temperatures T , which are subsequently used to extract charge gaps at low temperatures. This generalization results in the appearance of an extra phase factor in the expansion of the determinant ratios, which reduces to unity in the particle-hole symmetric system.

The rest of the paper is organized as follows. First, we briefly describe the imaginary chemical potential QMC (ICPQMC) formalism. Then simulation results on some Hubbard molecules are presented to illustrate

our method. The results are compared with the data obtained by exact diagonalization (ED) on small molecules and projector QMC (PQMC) on larger ones.

II. METHODOLOGY

We start with an expansion of the grand canonical partition function $Z_{GC}(\mu)$ in terms of canonical partition functions $Z_C(n)$ [6]:

$$Z_{GC}(\mu) = \text{Tr} e^{-(\hat{H} - \mu \hat{N})} = e^{-N\beta\mu} \sum_{n=-N}^N e^{n\beta\mu} Z_C(n); \quad (1)$$

where $\beta = 1/(k_B T)$ is the inverse temperature, μ is the chemical potential, n is the deviation of the particle number from half-filling (positive or negative, denoting electron or hole doping, respectively) in canonical ensemble, \hat{N} is the electron number operator, and N is the number of spatial lattice sites in the system. \hat{H} is the usual one-band Hubbard Hamiltonian:

$$H = \sum_{\langle ij \rangle} t_{ij} (c_i^\dagger c_j + \text{h.c.}) + U \sum_i n_i n_{i\uparrow\downarrow} + \frac{U}{2} \sum_i n_i; \quad (2)$$

The summation in the hopping term t_{ij} is performed over all nearest-neighbor pairs of the Hubbard molecule. For the C_{60} molecule we have set $t_{ij} = t$ for the links between the pentagons and hexagons and $t_{ij} = 1.2t$ for the links between hexagons. In all other cases t_{ij} was set equal to t for all links, with t used as an energy unit. U is the on-site Coulomb repulsion (Hubbard) term, and an extra diagonal term has been added to the Hamiltonian so that $\mu = 0$ corresponds to half-filling on bipartite lattices.

Following Dagotto et al. [6], we analytically continue Eq. (1) to imaginary chemical potential $\mu = i\phi$, where ϕ is real. Then the inverse Fourier transform of Eq. (1) gives

$$Z_C(n) = \frac{1}{2\pi} \int_0^{2\pi} d\phi e^{i\phi(n+N)} Z_{GC}(\mu = i\phi); \quad (3)$$

In AFQMC the grand canonical partition function is

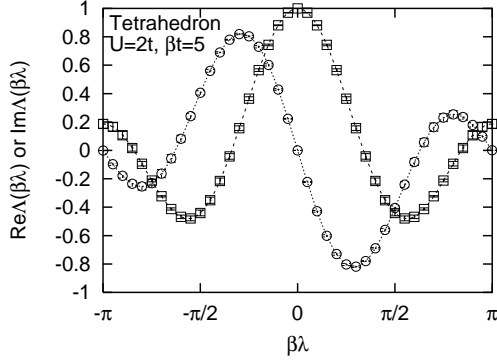


FIG. 1: Fit of real (squares) and imaginary (circles) parts of determinant ratios according to Eq. (12) for a tetrahedron molecule.

given by

$$Z_{GC}(\beta) = \frac{1}{\mathcal{Z}} \sum_{\{f, g\}} \det[1 + B_L(\beta)] B_{L-1}(\beta) \quad (13)$$

$$= \frac{\det O(f, g; \beta) \det O(f, g; \beta)_{\#}}{\det O(f, g; 0) \det O(f, g; 0)_{\#}}; \quad (4)$$

where the fermion degrees of freedom have been traced out, and the B_L matrices are defined as

$$B_L(\beta) = e^{-\sum_{ij} K_{ij} V_{ij}(\beta)}; \quad (5)$$

$$(K)_{ij} = \begin{cases} t_{ij} & \text{for } i, j \text{ nearest neighbors;} \\ 0 & \text{otherwise;} \end{cases} \quad (6)$$

$$V_{ij}(\beta) = -\ln[1 + e^{-\beta t_{ij}}]; \quad (7)$$

Here β is the imaginary time discretization interval and $\tanh^2(\beta/2) = \tanh(\beta/4)$. Thus, the original problem of taking a trace over fermionic degrees of freedom has been replaced by a problem of tracing over auxiliary Ising variables $\sigma_i(\beta)$, introduced at every space-time point $(i; \beta)$. Inserting Eq. (4) into Eq. (3), we get

$$Z_C(n) = \frac{1}{\mathcal{Z}} \sum_{\{f, g\}} \frac{Z_2}{2} \int_0^1 d\epsilon e^{i(n+N)\epsilon} \frac{\det O(f, g; i) \det O(f, g; i)_{\#}}{\det O(f, g; 0) \det O(f, g; 0)_{\#}}; \quad (8)$$

Dividing Eq. (8) by $Z_{GC}(\beta=0)$ from Eq. (4) yields

$$\frac{Z_C(n)}{Z_{GC}(0)} = \frac{1}{\mathcal{Z}} \sum_{\{f, g\}} P(f, g; 0) \frac{Z_2}{2} \int_0^1 d\epsilon e^{i n \epsilon} \quad (9)$$

where

$$P(f, g; 0) = e^{i N \epsilon} \frac{\det O(f, g; i) \det O(f, g; i)_{\#}}{\det O(f, g; 0) \det O(f, g; 0)_{\#}}; \quad (10)$$

and

$$P(f, g; 0) = \frac{\det O(f, g; 0) \det O(f, g; 0)_{\#}}{\mathcal{Z} \det O(f, g; 0) \det O(f, g; 0)_{\#}} \quad (11)$$

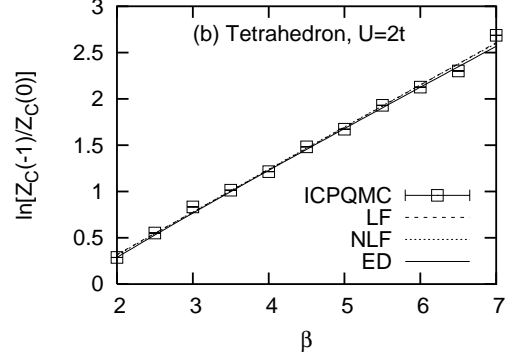
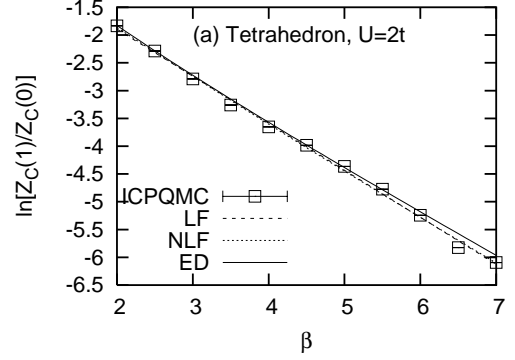


FIG. 2: Fits of ICPQMC data for a tetrahedron molecule at low temperatures for electron (a) and hole (b) doping. NLF forms for (a) and (b) are given by Eq. (14) and Eq. (15). ED results are also shown for comparison.

is the probability distribution for $Z_{GC}(0)$. Since there is always an energy gap above and below half-filling for any finite system, we expect the fermion determinants to be nearly β -independent at low temperatures. Therefore, we can generate the Ising field configurations f, g for $\beta=0$ and use these configurations to calculate system properties at $\beta \neq 0$.

Similar to the expansion in Eq. (1), we expect that the determinant ratio $\chi(\beta)$ in Eq. (10) can be expressed as complex Fourier series in the particle number n

$$\chi(\beta) = c_0(f, g) + \sum_{n=1}^N [c_n(f, g) + c_{-n}(f, g)] \cos(n\beta) + i \sum_{n=1}^N [c_n(f, g) - c_{-n}(f, g)] \sin(n\beta); \quad (12)$$

where $n(\beta)$ represents a doping of n electrons (holes) with respect to half-filling. Eq. (12) is real for systems with particle-hole symmetry, since then $c_n(f, g) = c_{-n}(f, g)$. When we substitute Eq. (12) back into Eq. (9), we see that $Z_C(n) = Z_{GC}(0) = \langle h_{n,i} \rangle$, where the average $\langle \cdot \rangle$ is over the Ising field configurations f, g generated from the probability distribution $P(f, g; 0)$. In the case of negative weight we replace P by its absolute value $|P|$ and include a sign $S = P/|P|$ in the average: $Z_C(n) = Z_{GC}(0) = \langle h_{n,i} S_i \rangle$. The average $\langle \cdot \rangle$

		LF	NLF	ED (PQMC)
C_4 ($U = 2t$)	$1;0$	0.85 (1)	0.87 (2)	0.82843
	$1;0$	-0.458 (9)	-0.358 (9)	-0.34949
	$2;1$	1.9 (1)	2.0 (1)	2.0
	$2;1$	-0.400 (6)	-0.397 (6)	-0.40466
C_8 ($U = 4t$)	$1;0$	1.20 (2)	1.27 (2)	1.26224
	$2;1$	1.44 (3)	1.5 (2)	1.27490
C_{12} ($U = 2t$)	$1;0$	0.81 (1)	0.997 (7)	0.99596
	$1;0$	0.041 (1)	0.10 (1)	0.07408
C_{60} ($U = 4t$)	$1;0$	0.43 (5)	0.57 (3)	0.561 (7)
	$1;0$	0.9 (1)	0.88 (4)	0.86 (2)

TABLE I: ICPQMC results on tetrahedron (C_4), cube (C_8), truncated tetrahedron (C_{12}) and C_{60} molecules. $n;0 = E(n) - E(0)$ is the energy difference between the ground states of the two fillings. Data marked by * are PQMC results, as described in Section IIIB.

now refers to the probability distribution \mathcal{P}_j . As we are interested in regions near half-filling, the sign problem does not limit the applicability of our method.

At low temperatures the canonical partition function ratio will be dominated by $n;0 = E(n) - E(0)$, the energy difference between the ground states for the two fillings, and will take the form [6]

$$\frac{Z_C(n)}{Z_C(0)} = \frac{hc_n i}{hc_0 i} \approx \frac{d_{n;0}}{d_{0;0}} e^{-\beta E_{n;0}} \quad \text{as } \beta \rightarrow \infty; \quad (13)$$

where $d_{n;0} = d_n = d_0$, with d_n being the degeneracy of the ground state at filling n . When there is an energy level close to the ground state (produced by the elementary excitations such as spin waves), we include it explicitly in the fitting expressions:

$$\frac{Z_C(n)}{Z_C(0)} = \frac{hc_n i}{hc_0 i} \approx \frac{d_{n;0} e^{-\beta E_{n;0}} + f_{n;0} e^{-\beta E_{sw}^n}}{1 + f_{0;0} e^{-\beta E_{sw}^0}} \quad \text{as } \beta \rightarrow \infty; \quad (14)$$

Here $f_{n;0} = \frac{d_{sw}^n}{d_{sw}^0}$, where d_{sw}^n is the degeneracy of the spin wave state at filling n , and $E_{sw}^n = E_{sw}(n) - E(0)$ are the spin-wave gaps at filling n with respect to the ground state at half-filling.

Based on the above discussion, we formulate the following calculation procedure:

1. Generate the Ising field configuration \mathbf{f}_g according to the probability distribution $P(\mathbf{f}_g; 0)$ in the AFQMC simulation of $Z_{GC}(0)$.
2. Evaluate the average of the determinant ratio on the left-hand side of Eq. (12) over the Ising field configurations for a set of β values.
3. Fit the real and imaginary parts of Eq. (12) respectively to determine the average values of $hc_n i$, $n = 0; 1; 2; \dots$. From now on we will refer to these values simply as c_n .

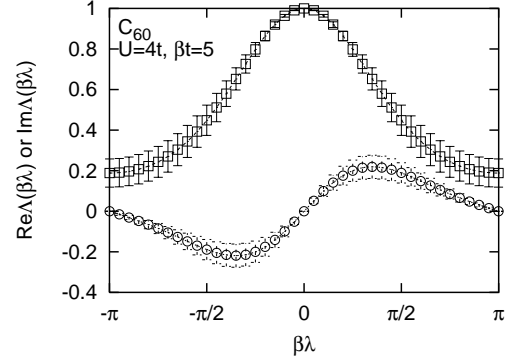


FIG. 3: Fits of the real (squares) and imaginary (circles) parts of determinant ratios according to Eq. (12) for a C_{60} molecule.

4. Fit the canonical partition function ratios $Z_C(n)/Z_C(0) = c_n/c_0$, $n = 1; 2; \dots$ with low temperature canonical partition function ratio expressions (13) or (14) to obtain energy gaps. Below we will refer to these fits as linear (LF) and non-linear (NLF), respectively.

III. APPLICATION

ICPQMC simulations have been carried out on tetrahedron, cube, truncated tetrahedron and C_{60} molecules. For each molecule, we have run the simulations at temperatures $t = 2.0; 2.5; \dots; 6.5; 7.0$. The imaginary chemical potential i was chosen so that $0 < \beta \lambda < \pi$, and we used a set of 20 evenly distributed $\beta \lambda$ values in this range. We have numerically checked that the real part of Eq. (12) is an even function around $\beta \lambda = 0$, while the imaginary part is odd. Using this property, we have mapped out the determinant ratio data for $\beta \lambda > 0$. For the special particle-hole symmetric case, such as a 2D square lattice, we have tested our programs for the 2×2 and 4×4 systems, reproducing the results of Ref. [6].

A. Tetrahedron, Cube and Truncated Tetrahedron

Fig. 1 displays the fit of the real and imaginary parts of Eq. (12) for a tetrahedron molecule (C_4). Similar fits were performed for data at all temperatures, generating a set of coefficients c_n . Knowledge of these coefficients enables us to calculate the partition function ratios at various temperatures, and, at low temperatures, to linearly fit the logarithm of these ratios to obtain the energy gaps and degeneracy ratios. Results of this procedure are presented in Fig. 2 and Table I. We see that $c_{2;1}$ and $c_{2;1}$ from LF agree nicely with ED, while $c_{1;0}$ does not. A likely cause of this discrepancy is the existence of a highly degenerate ($d_{sw}^0 = 9$) spin wave energy level very close ($E_{sw}^0 = 0.14258t$) to the ground state ($d_0 = 2$) at half-filling. Results of the fits for electron ($n = 1$) and

hole ($n = 1$) doping are presented in Figs. 2a and 2b respectively. The NLFs were obtained using form (14) by fixing the spin wave and degeneracy parameters to the values found by ED :

$$\begin{aligned} f_{1;0} &= 3; & \frac{1}{SW} &= 1:18268t; \\ f_{0;0} &= 4.5; & \frac{0}{SW} &= 0:14258t; \end{aligned} \quad (15)$$

In the case of hole doping the spin wave term proportional to $f_{1;0}$ in the numerator of Eq. (14) has been neglected.

Examining Fig. 2 we find that inclusion of spin waves does not make a substantial difference: LF and NLF curves are nearly overlapping [with a slight difference around $t = 2$ for $\ln(Z_C(1)/Z_C(0))$] and are very close to the exact values. This insensitivity to the fitting parameters makes accurate extraction of energy gaps from partition function ratios difficult.

Analogous simulations and LF/NLF fittings were performed for cube (C_8) and truncated tetrahedron (C_{12}) molecules. The energy gaps measured using this procedure are summarized in Table I. The fitting procedure for C_{60} is described below.

B. C_{60}

Fig. 3 shows a plot of the real and imaginary parts of Eq. (12) for a C_{60} molecule. The imaginary parts of the determinant ratios are positive for $\beta > 0$, which is different from the tetrahedron and truncated tetrahedron cases. The cause of this difference is the relative size of electron and hole gaps in the system. The larger the gaps, the smaller the corresponding canonical partition function ratios $Z_C(n)/Z_C(0)$. For the tetrahedron and the truncated tetrahedron the electron gaps are larger than the hole gaps, so $c_1 < c_{-1}$. In contrast, for the C_{60} molecule the electron gap is smaller than the hole gap, so $c_1 > c_{-1}$. Therefore, the relative size of the canonical partition function ratios results in a positive imaginary part of the determinant ratios for $\beta > 0$ in Fig. 3 due to Eq. (12). Similar tests were done for other temperatures, and the resulting canonical partition function parameters c_n were obtained to calculate the canonical partition function ratios. Unfortunately, Eq. (14) contains too many fitting parameters to provide unique fits to the data. Therefore, we had to rely on the PQMC results (at $U = 4t$) for the gap values

$$\begin{aligned} \frac{1}{SW} &= 0:561t; & \frac{0}{SW} &= 1:06t; \\ \frac{1}{SW} &= 1:39t; & \frac{1}{SW} &= 1:54t; \end{aligned} \quad (16)$$

and on the analysis of the molecular orbital energy level diagram (Fig. 3 of Ref. 1) for the degeneracies and their ratios

$$\begin{aligned} d_0 &= 1; & d_{1;0} &= 6; & d_{-1;0} &= 10; \\ f_{1;0} &= 120; & f_{-1;0} &= 10; & f_{0;0} &= 30; \end{aligned} \quad (17)$$

We were able to demonstrate the consistency of the results obtained by the two methods (ICPQMC and

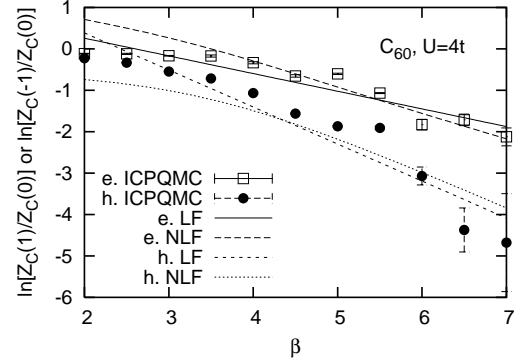


FIG. 4: Fits of ICPQMC data for a C_{60} molecule at low temperatures for electron and hole doping. e. (h.) denotes electron (hole) doping.

PQMC) by employing a following procedure. We first let all three gap values be free fitting parameters. Fitting results are then in agreement with the PQMC results, albeit with rather large uncertainties. Then we fix in the two PQMC gap values $\frac{1}{SW}$ and $\frac{0}{SW}$ [Eq. (16)], and let $\frac{1}{SW}$ be the only free parameter. This procedure, in general, yields the gap values consistent with the ones previously obtained using PQMC method [1]. Detailed results are presented in Table I with representative fits shown in Fig. 4.

IV. CONCLUSION

We have generalized the particle-hole symmetric ICPQMC simulation of Dagotto et al. [6] to systems without this symmetry, such as the tetrahedron, truncated tetrahedron, and C_{60} molecule. Our simulations show that an accurate canonical partition function ratio can be obtained through this technique. Unfortunately, the fitting of these ratios to obtain accurate energy gaps for C_{60} is impractical. Nevertheless, consistency between ED, PQMC and ICPQMC has been found.

Acknowledgments

FL thanks Graeme Luke for helpful advice on figure preparation. We gratefully acknowledge the support of this project by Natural Sciences and Engineering Research Council (Canada), The Canadian Institute for Advanced Research (CIAR), CFI and SHARCNET. All the calculations were carried out at SHARCNET supercomputing facilities at McMaster University.

-
- [1] F. Lin, J. Smakov, E.S. Sørensen, C. Kallin and A.J. Berlinsky, cond-mat/0411422 (2004).
- [2] R. Blankenbecler, D.J. Scalapino and R.L. Sugar, Phys. Rev. D 24, 2278 (1981).
- [3] D.J. Scalapino and R.L. Sugar, Phys. Rev. B 24, 4295 (1981).
- [4] J.E. Hirsch, Phys. Rev. B 28, R4059 (1983); 29, 4159 (E) (1984); 31, 4403 (1985); Phys. Rev. Lett. 51, 1900 (1983).
- [5] S.R. White et al., Phys. Rev. B 40, 506 (1989).
- [6] E. Dagotto, A. Moreo, R.L. Sugar and D. Toussaint, Phys. Rev. B 41, R811 (1990).